

Formation, Spectroscopy, Photochemistry, and Quantum Chemistry of the (S₂)(O₂) Complex in Solid Argon

G. Dana Brabson,[†] Angelo Citra,[†] Lester Andrews,^{*,†} Randall D. Davy,[‡] and Matthew Neurock[§]

Contribution from the Department of Chemistry and the Department of Chemical Engineering, University of Virginia, Charlottesville, Virginia 22901, and the Department of Chemistry, Liberty University, Lynchburg, Virginia 24506

Received February 14, 1996[⊗]

Abstract: Samples formed by codepositing S₂ from a superheater source with Ar/O₂ on a 10 K substrate exhibit very strong 1403.0-cm⁻¹ and weaker 725.5-cm⁻¹ infrared absorptions. Photolysis decreases these bands slightly and produces SO₂ and S₂O. The infrared bands show ¹⁸O₂ and ³⁴S₂ shifts appropriate for O–O and S–S fundamental vibrations, and triplet absorptions in mixed isotopic experiments suggesting two equivalent O and two equivalent S atoms in the product complex. Similar results were obtained for Se₂ and O₂; new absorptions appeared at 1404.5 and 391 cm⁻¹. Ab initio calculations at the SCF, CISD, and CCSD levels of theory failed to find a complex with the observed spectroscopic properties. However, calculations with the BP density functional characterized a singlet (S₂)(O₂) parallelogram structure bound by 15.6 kJ/mol relative to triplet S₂ and O₂ with the O–O stretching frequency red-shifted 187 cm⁻¹ and the S–S fundamental blue-shifted 20 cm⁻¹. This weakly bound (S₂)(O₂) complex is chemically intermediate between the unstable O₄ and stable S₄ molecules. The argon matrix has made possible the formation of the weak (S₂)(O₂) complex and DFT with the BP functional has characterized this weak charge-transfer interaction.

Introduction

The existence of a weakly-bonded, dimeric O₄ molecule has been considered from paramagnetic susceptibility,¹ crystal structure,² electronic spectroscopy,³ and chemiluminescence⁴ measurements on oxygen. Pauling even gives some credence to the possibility of a weakly bound O₄ molecule.⁵ However, infrared studies of solid oxygen, including isotopic mixtures, found no evidence for dimeric (O₂)₂ molecules.⁶ Subsequent spectroscopic studies of the Van der Waals (O₂)₂ dimer in the gas phase around 90 K and in solid neon at 4 K show that the dimer vibrational fundamentals are unperturbed from the gas-phase O₂ fundamental.^{7,8} Very recent electron-transfer experiments with O₄⁺ have formed short-lived electronic states of O₄ at 26 kcal/mol above O₂ + O₂.⁹ Finally, theoretical investigations have found a physically stable puckered O₄ ring of D_{2d} symmetry containing normal single bonds, but this energetic O₄ molecule is calculated at the highest level of theory to be 83 kcal/mol above 2O₂ molecules.^{10–12}

On the other hand, S₄ is a stable molecular species, and evidence for two different structural isomers has been presented

in matrix isolation and gas-phase studies.^{13–17} A reversible photoisomerization has been documented for these two S₄ isomers; analogous behavior has been reported for Se₄ and Te₄.^{14,18,19} Recent high-level theoretical studies have shown that *cis*-S₄ is the minimum energy structure,²⁰ but rectangular S₄ is very close in energy.^{21,22}

What then is the possibility for a similar S₂O₂ molecule? Apparently the most stable isomer is *cis*-OSSO, which was characterized by microwave spectroscopy in an electric discharge through SO₂.²³ During earlier work with small sulfur and selenium clusters in this laboratory, weak bands persisted near 1400 cm⁻¹.^{13,18} When O₂ was added to the argon matrix gas these bands increased markedly. The new bands near 1400 cm⁻¹ form the basis for the present investigation of S₂O₂ and Se₂O₂ complex rings.

Experimental Section

The matrix isolation apparatus and sulfur and selenium superheater sources have been described previously.^{13,18} Sulfur (Electronic Space Products, Inc., natural abundance, recrystallized), Se (Alpha, m3N,

(13) Brabson, G. D.; Mielke, Z.; Andrews, L. *J. Phys. Chem.* **1991**, *95*, 79.

(14) Hassanzadeh, P.; Andrews, L. *J. Phys. Chem.* **1992**, *96*, 6579.

(15) Meyer, B.; Oommen, T. V.; Jansen, D. J. *J. Phys. Chem.* **1971**, *75*, 912. Meyer, B.; Stroyer-Hansen, T.; Oommen, T. V. *J. Mol. Spectrosc.* **1972**, *42*, 335.

(16) Steudel, R.; Jensen, D.; Godel, P. *Ber. Bunsen-Ges. Phys. Chem.* **1988**, *92*, 118.

(17) Lenaine, P.; Picquenard, E.; Corset, J.; Jensen, D.; Steudel, R. *Ber. Bunsen-Ges. Phys. Chem.* **1988**, *92*, 859.

(18) Brabson, G. D.; Andrews, L. *J. Phys. Chem.* **1992**, *96*, 9172.

(19) Hassanzadeh, P.; Thompson, C. A.; Andrews, L. *J. Phys. Chem.* **1992**, *96*, 8246.

(20) Quelch, G. E.; Schaeffer, H. F., III; Marsden, C. J. *J. Am. Chem. Soc.* **1990**, *112*, 8719.

(21) Raghavachari, K.; Rohlfing, C. M.; Binkley, J. S. *J. Chem. Phys.* **1990**, *93*, 5862.

(22) Von Niessen, W. *J. Chem. Phys.* **1991**, *95*, 8301.

(23) Lovas, F. J.; Tiemann, E.; Johnson, D. R. *J. Chem. Phys.* **1974**, *60*, 5005.

[†] Department of Chemistry, University of Virginia.

[‡] Liberty University.

[§] Department of Chemical Engineering, University of Virginia.

[⊗] Abstract published in *Advance ACS Abstracts*, May 15, 1996.

(1) Lewis, G. N. *J. Am. Chem. Soc.* **1924**, *46*, 2027.

(2) Vegard, L. *Nature* **1935**, *136*, 720.

(3) Cho, C. W.; Allin, E. J.; Welsh, H. L. *Can. J. Phys.* **1963**, *41*, 1991.

(4) Arnold, S. J.; Ogryzlo, E. A.; Witzke, H. *J. Chem. Phys.* **1964**, *40*, 1769.

(5) Pauling, L. *The Nature of the Chemical Bond*, 3rd ed.; Cornell University Press: Ithaca, NY, 1960.

(6) Cairns, B. R.; Pimentel, G. C. *J. Chem. Phys.* **1965**, *43*, 3432.

(7) Long, C. A.; Ewing, G. E. *J. Chem. Phys.* **1973**, *58*, 4824.

(8) Goodman, J.; Brus, L. E. *J. Chem. Phys.* **1977**, *67*, 4398.

(9) Helm, H.; Walter, C. W. *J. Chem. Phys.* **1993**, *98*, 5444.

(10) Seidl, E. T.; Schaeffer, H. F., III *J. Chem. Phys.* **1988**, *88*, 7043.

(11) Dunn, K. M.; Scuseria, G. E.; Schaeffer, H. F., III *J. Chem. Phys.* **1990**, *92*, 6077.

(12) Seidl, E. T.; Schaeffer, H. F., III *J. Chem. Phys.* **1992**, *96*, 1176.

natural abundance, 325 mesh powder), natural abundance oxygen (Matheson), scrambled $^{16,18}\text{O}_2$ (YEDA, 53.1 atom % ^{18}O), and $^{18}\text{O}_2$ (YEDA, 97.5 atom % ^{18}O) were used as received. In the infrared experiments, argon–oxygen (1.0 to 0.1%) samples were codeposited with S_2 or Se_2 on a CsI window at 12 ± 1 K, and spectra were recorded with a Perkin-Elmer 983 spectrophotometer from 2500 to 180 cm^{-1} at a resolution of 1 cm^{-1} and a wavenumber accuracy of $\pm 0.5\text{ cm}^{-1}$. In the UV–visible experiments, samples were collected on a sapphire window at 17 ± 3 K, and spectra were recorded on a Cary 17 spectrophotometer from 850 to 250 nm with a resolution of 1 nm and a wavelength accuracy of ± 0.1 nm. Photolysis experiments were performed using the filtered light from a high-pressure mercury arc (B-H6, T.J. Sales). A water cell was used to absorb infrared radiation and thereby minimize heating of the sample. To selectively irradiate the sample with UV light from 235 to 360 nm, a Corning No. 9863 filter (which blocks visible light) was used in tandem with a saturated solution of cobalt acetate. In the annealing experiments, the sample was exposed to a series of successively higher temperatures; the sample was quenched and the spectrum was scanned after each temperature excursion.

The quartz superheated Knudsen cell was located entirely inside the vacuum chamber. The vapor density in the Knudsen cell was controlled by setting the temperature of the reservoir; thermal fragmentation was achieved in the superheated zone at a nominal temperature of $900\text{ }^\circ\text{C}$ (estimated by optical pyrometry). For infrared experiments, the best results were obtained with a reservoir temperature of $70\text{--}85\text{ }^\circ\text{C}$ for sulfur and $120\text{--}130\text{ }^\circ\text{C}$ for selenium and a total deposition time of $8\text{--}10$ h at a rate of about 2.5 mmol/h of argon matrix gas. The amount of Se_2 in the matrix was monitored by following the Se_2 fine-structure band at 513 cm^{-1} .¹⁸ The best results were obtained when the 513 cm^{-1} band was just barely visible in the spectra; under these conditions, the Se_4 bands at 370 and 345 cm^{-1} were weak or not observed. By comparison with prior work on Se_3 and Se_4 clusters,¹⁸ the vapor pressure of selenium in the present experiments was 1–2 orders of magnitude smaller. For the UV–visible experiments, still less Se_2 was needed; a typical reservoir temperature was $110\text{ }^\circ\text{C}$, deposition times were about 1 h, and the concentration of Se_2 was monitored by observing the UV band system ($310\text{--}377\text{ nm}$).

Results

Matrix isolation experiments will be presented for sulfur and selenium with oxygen.

Sulfur and Oxygen. Codeposition of S_2 and O_2 in excess argon results in two very sharp bands, a strong band at 1403.0 cm^{-1} (fwhm = 1.0 cm^{-1}) and a weaker band at 725.5 cm^{-1} (fwhm = 0.7 cm^{-1} , relative absorbance = 6/1), as shown in Figure 1a. The 1403.0 cm^{-1} band has satellites at 1408 , 1405 , and 1400 cm^{-1} , whose behavior under photolysis and annealing is slightly different from that of the principal band, suggesting that these satellites are due to different trapping sites. The 725.5 cm^{-1} band is undoubtedly the band reported at 725.7 cm^{-1} and at that time tentatively assigned to an $\text{S}_2\text{--H}_2\text{O}$ complex.¹³ This band shifted to 704.1 cm^{-1} with ^{34}S and showed a 1/2/1 triplet at 725.5 , 714.9 , and 704.1 cm^{-1} with mixed $^{32,34}\text{S}$ isotopic sulfur.¹³ The conclusion that the 1403.0 - and 725.5 cm^{-1} bands should be assigned to the same molecule is strongly supported by the fact that these are the only two bands which show dramatic enhancements on addition of O_2 to the argon matrix gas, and by the observation that these two bands track under all experimental conditions including photolysis and annealing.

A similar reaction with $^{18}\text{O}_2$ shifted the strong band to 1324.2 cm^{-1} with a 1329 -, 1326 -, and 1321 cm^{-1} satellite and the 725.5 cm^{-1} band was not shifted (Figure 1c); a small amount of $^{16}\text{O}_2$ was present in the $^{18}\text{O}_2$ sample. In $^{16,18}\text{O}_2$ experiments, the O–O vibration displayed a sharp 1/2/1 triplet at 1403.0 , 1364.1 , and 1324.2 cm^{-1} , which is shown in Figure 2b (satellites not observed at this signal to noise).

The only sulfur oxide observed in the initial deposit was isolated SO_2 evidenced by sharp weak bands at 1354.7 and

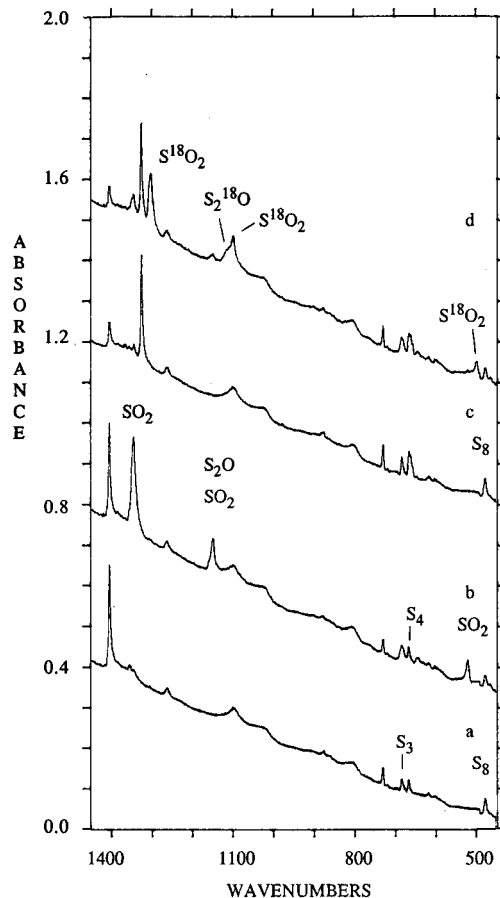


Figure 1. Infrared spectra in the $1450\text{--}450\text{ cm}^{-1}$ region for S_2 codeposited from superheater with $\text{Ar}/\text{O}_2 = 400/1$ samples for 6 h: (a) $\text{S}_2 + ^{16}\text{O}_2$ in excess argon, (b) spectra after final full-arc photolysis, (c) $\text{S}_2 + ^{18}\text{O}_2$ in excess argon, and (d) spectra after final full-arc photolysis.

1350.9 cm^{-1} . Photolysis was done in stages with long-wavelength pass filters, $\lambda > 490$, $\lambda > 380$, $\lambda > 290$, and full-arc, and the decrease of 1403 - and 725 cm^{-1} bands and growth of 1347 -, 1344 -, 1147 -, and 519 cm^{-1} bands was observed at 10%, 10%, and 70% of the final full arc effect with the above filters, respectively. The 1403 - and 725 cm^{-1} bands decreased by 20% and the S_4 band at 661 cm^{-1} decreased while the S_4 band at 642 cm^{-1} increased, as reported previously. Spectra before and after photolysis are shown in Figure 1a,b for the $^{16}\text{O}_2$ photoproducts. The new bands at 1347 , 1344 , 1147 , and 519 cm^{-1} are due to SO_2 , but in this case, the molecule appears to be perturbed by other species in the matrix. A different photolysis sequence was employed in another experiment. A $265 < \lambda < 360\text{ nm}$ notch filter increased the S_3 and S_4 bands, and produced very weak product bands, but a wider notch $235 < \lambda < 360\text{ nm}$ reduced 1403 - and 725 cm^{-1} bands by 5% and produced the 1344 -, 1147 -, and 519 cm^{-1} product bands. Final full arc photolysis reduced 1403 - and 725 cm^{-1} bands by 10%, and increased the product bands 4-fold: 1344 ($A = 0.15$), 1147 ($A = 0.06$), and 519 cm^{-1} ($A = 0.03$). Product absorptions are collected in Table 1.

Convincing evidence for this assignment includes the data from $^{18}\text{O}_2$ experiments shown in Figure 1c,d, which gives new photolysis product bands at 1305 , 1301 , 1106 shoulder, 1097 , and 497 cm^{-1} . The observed intensity of the 1147 cm^{-1} band in Figure 1b is too large to attribute this band entirely to SO_2 . The second contributing molecule at this energy is a perturbed S_2O , and its corresponding oxygen-18 band is at 1106 cm^{-1} ; again, the isotopic shift and the absence of a mixed isotopic component are in accord with expectation for S_2O . In the $^{16,18}\text{O}_2$

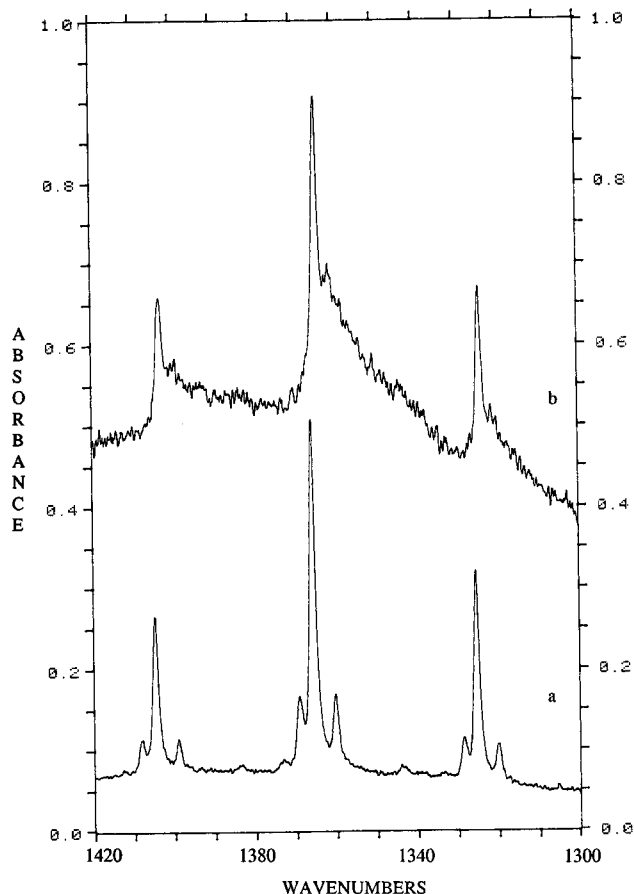


Figure 2. Infrared spectra in the 1420–1300-cm⁻¹ region for (a) Se₂ and (b) S₂ codeposited with an Ar/^{16,18}O₂ = 400/1 sample for 8 h.

Table 1. Infrared Absorptions (cm⁻¹) Observed on Codeposition of S₂ with O₂ in Excess Argon at 12 K

S ₂ + ¹⁶ O ₂	after photolysis	S ₂ + ¹⁸ O ₂	after photolysis
1408			1329
1405		1326	
1403.0	dec	1324.2	dec
1400		1321	
1354.7 (SO ₂)	1347 (SO ₂)		1305 (S ¹⁸ O ₂)
1350.9 (SO ₂)	1344		1301
	1147 (SO ₂ , S ₂ O)		1106 (S ₂ 18O)
			1097 (S ¹⁸ O ₂)
725.5	dec	725.5	dec
676 (S ₃)		676 (S ₃)	
661 (S ₄)		661 (S ₄)	
642 (S ₄)		642 (S ₄)	
	519 (SO ₂)		497 (S ¹⁸ O ₂)
474 (S ₈)		474 (S ₈)	

experiment, the product bands are 1344, 1327, 1302 cm⁻¹ and 1147, 1118, 1097 cm⁻¹ for SO₂ and 1147, 1106 cm⁻¹ for S₂O, with 1106 cm⁻¹ stronger than 1118 cm⁻¹ absorption. In discharge experiments, S₂¹⁶O absorbs at 1157.0 cm⁻¹ and S₂¹⁸O at 1115.5 cm⁻¹.

Given the observed photolysis behavior, the UV-visible spectrum was explored, and a strong featureless absorption was found, extending from 240 to 300 nm, with distinct absorption maxima at 259 and 276 nm. In these experiments, the temperature of the sulfur reservoir (ca. 40 °C) was much lower than that required for typical IR experiments; under these conditions, the banded S₂ spectrum²⁴ was not observed, nor were any of the systems known to belong to S₃ or S₄.¹⁴ By increasing

Table 2. Infrared Absorptions (cm⁻¹) Observed on Codeposition of Se₂ with O₂ in Excess Argon at 12 K

Se ₂ + ¹⁶ O ₂	Se ₂ + ¹⁶ O ¹⁸ O	Se ₂ + ¹⁸ O ₂
1407.7	1368.6	1328.2
1404.5	1365.4	1325.2
1399.0	1360.0	1320.0
1372.4	1334.3	1295.1
391	391	391

the sulfur reservoir temperature to about 80 °C, both the broad absorption pattern and the banded S₂ spectrum were easily obtained, with the S₂ spectrum being superimposed on the long-wavelength half of the broad absorption pattern. The photolysis behavior of the broad absorption pattern paralleled that of the infrared bands at 1403 and 725 cm⁻¹, and this broad absorption is, therefore, due to the same species.

Selenium and Oxygen. Codeposition of Se₂ from a superheated Knudsen cell and O₂ yields a strong, sharp band at 1404.5 cm⁻¹ with well-resolved satellites at 1399.0 and 1407.7 cm⁻¹, a weak, sharp band at 1372.4 cm⁻¹, and a broad weaker band at 391 cm⁻¹. Based on the fact that the 1404.5- and 391-cm⁻¹ bands track together through all experimental conditions, they are assigned to the same species. The 1404.5-cm⁻¹ band is sharp (fwhm = 1.7 cm⁻¹), while the 390-cm⁻¹ band is much broader (fwhm = 9 cm⁻¹); the relative integrated absorbances of these bands are 15:1. Although the location of the 1404.5-cm⁻¹ band is close to that of the corresponding sulfur band, it is clearly different, being 1.5 cm⁻¹ to the blue and having a uniquely different set of satellite bands.

Experiments with ¹⁸O₂ shifted the strong band to 1325.2 cm⁻¹ and the satellites as listed in Table 2. Figure 2a shows the strong, sharp 1/2/1 triplet observed at 1404.5, 1365.4, and 1325.2 cm⁻¹ with equivalent sets of isotopic satellites.

In contrast to the sulfur system, visible photolysis (λ > 490 nm) decreased the 1404.5- and 391-cm⁻¹ bands and produced new bands at 966, 959, 921, 637, and 366 cm⁻¹ and ultraviolet photolysis (235 < λ < 360 nm) further decreased the 1404.5- and 391-cm⁻¹ bands and produced a new 876-cm⁻¹ band. These Se_xO_y bands will be identified in a later study including ozone and microwave discharge reaction products. The 959-, 921-, and 366-cm⁻¹ photoproducts are clearly due to perturbed SeO₂.²⁵

In the ultraviolet, a broad featureless absorption with two maxima was found, extending from 235 to 310 nm, but not overlapped by the Se₂ band system,¹⁸ which lies between 310 and 377 nm. Both the broad featureless absorption and the banded Se₂ system were easily obtained under the same experimental conditions. The two absorption maxima at 256 and 293 nm were separated by a larger wavelength interval than in the sulfur-oxygen system; indeed, the UV spectrum for the selenium-oxygen system can be described in terms of two independent features. Note that the shorter-wavelength features in the sulfur and selenium systems are both at similar wavelengths, while the longer-wavelength features display a considerable difference, with the selenium-oxygen feature at longer wavelengths. This is, of course, in accord with the hypothesis that this longer-wavelength feature can be assigned to an electronic transition dominated by the Se₂ chromophore and the shorter-wavelength feature is dominated by the O₂ chromophore.

Calculations

Initially a search was made for a weak O₂-S₂ complex with equivalent oxygens using ab initio self-consistent field (SCF) calculations with DZP and TZ2P basis sets. Several S₂-O₂ structures were

(24) Brewer, L.; Brabson, G. D.; Meyer, B. *J. Chem. Phys.* **1965**, *42*, 1385.

(25) Brabson, G. D.; Andrews, L.; Marsden, C. To be submitted for publication.

investigated, but either were dissociative or strongly bound and shifted $\Delta\nu(\text{OO})$ by more than 800 cm^{-1} . A C_{2v} structure was found with (SCF/TZ2P): $\Delta\nu(\text{OO})$ of -383 cm^{-1} , $\Delta\nu(\text{SS})$ of $+30\text{ cm}^{-1}$, and $\text{O}-\text{O} = 1.207\text{ \AA}$, $\text{S}-\text{S} = 1.820\text{ \AA}$, and $\text{S}-\text{O} = 1.820\text{ \AA}$. This structure, however, is high energy ($+111\text{ kcal/mol}$ above free S_2 and O_2 at the SCF/TZ2P level) and not a minimum. It possesses an imaginary frequency along a mode that leads to a *cis*-OOSS open chain. The SCF method, however, favors the triplet fragments energetically. Including correlation at the CISD/DZP and CCSD/DZP levels decreased the relative energy of the C_{2v} ring versus free S_2 and O_2 to 60 and 37 kcal/mol, respectively. At the CISD/DZP level the frequency shifts are $\Delta\nu(\text{OO})$ of -200 cm^{-1} and $\Delta\nu(\text{SS})$ of $+60\text{ cm}^{-1}$. Thus there is a reasonable match between experimental frequency shifts and those obtained at both the CISD/DZP and SCF/DZP for the C_{2v} ring, and its relative energy decreases as the level of theory is increased. The theoretical methods based on a single determinant (i.e. SCF, CISD, CCSD) obtain a high energy for the C_{2v} structure and an imaginary frequency leading to the lower energy *cis*-OOSS structure due to an underlying symmetry breaking problem common to systems with partial donation of an electron into O_2 , for example LiO_2 .²⁶ One could move to a multireference correlated wave function, however density functional theory (DFT) is a less costly alternative approach.

In the SiNN case that proved difficult for SCF/CISD calculations, DFT produced results that match experimental results, which have been obtained by non-DFT multireference methods such as MRCCSD.^{27–30}

DFT calculations were performed on a variety of S_2O_2 structures using the DGauss program developed by Cray Research Inc.³¹ DGauss employs Gaussian basis sets to solve the single-particle Kohn–Sham equations.³² Local spin density exchange correlation is represented by the Vosko–Wilk–Nusair potential.³³ Non-local gradient corrections to the exchange and correlation are determined within the SCF cycle using the correlation and exchange potentials developed by Becke and Perdew (BP), respectively.^{34,35} DFT-optimized DZVP2 (721/51/1) basis sets were employed throughout.³⁶ All SCF calculations were converged to within 5×10^{-7} au on the SCF energy, and all structures were optimized to within 8×10^{-4} au/Å. Second derivatives, force constants, and frequencies were all determined analytically using the harmonic oscillator approximation.

DFT calculations with the BP functional predict O_2 complexes with sulfur made from ground triplet state S_2 and O_2 molecules. Several relative orientations were considered including parallel, T-shape, and head-to-head. When the complex was optimized using DFT/BP with an overall quintet state the result was the same regardless of initial orientations: the molecules separated—no complex was formed.

Second, triplet O_2 complexes with S_4 were examined using singlet S_4 in both C_{2v} and D_{2h} forms known to be low-energy structures. Again, no stable complex was formed. With cyclic S_4O_2 and a singlet state, the $\text{O}-\text{O}$ bond ruptured to give an OSSSSO species.

Third, O_2 complexes with S_2 having overall triplet and singlet spin states were explored using DFT/BP. The triplet complex was repulsive like the original quintet attempt. However, the overall singlet complex optimized in a stable parallelogram arrangement with shorter $\text{S}-\text{O}$ distances than any other complex investigated, and the total energy was 15.6 kJ/mol less than the sum of calculated ground state S_2 and O_2 energies. Figure 3 compares calculated bond lengths for the $(\text{S}_2)(\text{O}_2)$ complex and the S_2 and O_2 molecules; the $\text{O}-\text{O}$ bond length is increased and the $\text{S}-\text{S}$ bond length decreased in the complex. Correspondingly, the calculated $\text{O}-\text{O}$ frequency is red shifted 187 cm^{-1}

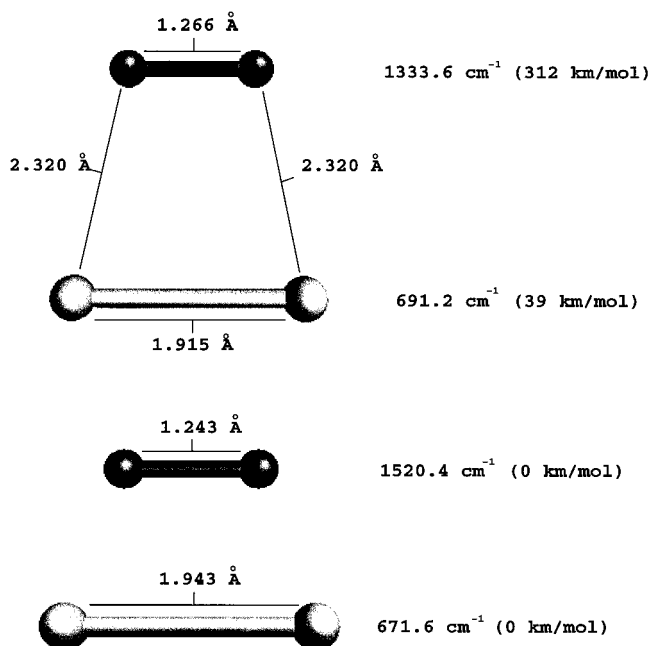


Figure 3. Calculated bond lengths and frequencies for the $(\text{S}_2)(\text{O}_2)$ complex using DFT/BP.

and the $\text{S}-\text{S}$ frequency blue shifted 20 cm^{-1} in the complex. These compare to the 149-cm^{-1} red shift in $\text{O}-\text{O}$ frequency and 10-cm^{-1} blue shift in $\text{S}-\text{S}$ frequency observed here for the $(\text{S}_2)(\text{O}_2)$ complex. A similar calculation with TZVP basis sets gave almost the same results: $\text{BE} = 15.0\text{ kJ/mol}$, $\Delta\nu(\text{OO}) = -192\text{ cm}^{-1}$, $\Delta\nu(\text{SS}) = +21\text{ cm}^{-1}$, $\text{S}-\text{O} = 2.284\text{ \AA}$. This indicates a flow of electron density from the $\text{S } 3\pi^*$ to the $\text{O } 2\pi^*$ antibonding molecular orbitals.

Two DFT calculations were done with G92/DFT and the D95++** basis sets at the San Diego Supercomputer Center. The first employed the hybrid B3LYP functional. A similar parallelogram $(\text{S}_2)(\text{O}_2)$ structure was obtained, and similar red-shifted (154 cm^{-1}) O_2 and blue-shifted (22 cm^{-1}) S_2 frequencies were found, but the singlet $(\text{S}_2)(\text{O}_2)$ energy was higher than the sum of triplet S_2 and O_2 by 88 kJ/mol . The second employed the pure BP 86 density functional. Again a similar parallelogram structure, 201-cm^{-1} red-shifted O_2 and 19-cm^{-1} blue-shifted S_2 , was found, and the singlet $(\text{S}_2)(\text{O}_2)$ energy was lower than the sum of triplet S_2 and O_2 by 22 kJ/mol . Apparently the pure BP density functional is required to find stability for the $(\text{S}_2)(\text{O}_2)$ complex. The discrepancy between the SCF/CISD/CCSD methods and DFT is unusual but has precedence as mentioned above in the case of SiNN. More remarkable is the difference between the pure and hybrid DFT methods in the present case. This difference is particularly important to note because of the tremendous growth in the use of DFT methods.

Similar test calculations were performed on O_4 and S_4 . In the former case, two parallel O_2 molecules were placed 1.7 \AA apart and then 2.1 \AA apart; these systems converged to rectangular structures with long dimensions of 1.991 and 1.994 \AA and total energies higher than those of 2O_2 by 42.2 kJ/mol . This structure gave $\text{O}=\text{O}$ stretching modes at 1506 and 1376 cm^{-1} . In the latter case, a rectangular S_4 isomer (1.936 and 2.647 \AA) was calculated lower in energy than 2S_2 by 85.8 kJ/mol and gave $\text{S}=\text{S}$ stretching modes at 678.4 (0 km/mol) and 637.6 cm^{-1} (108 km/mol) and a *cis*- C_{2v} S_4 isomer (1.944 , 2.282 \AA) was calculated lower in energy than 2S_2 by 83.5 kcal/mol and gave $\text{S}=\text{S}$ stretching modes at 653.1 (2 km/mol) and 628.4 cm^{-1} (106 km/mol). The frequencies calculated here are comparable to those from higher (CISD) levels of theory for the *cis* structure but lower by 150 – 200 cm^{-1} for the rectangular isomer. The more stable S_4 isomer absorbs at 662 cm^{-1} in solid argon.¹³

A molecular orbital diagram is shown for the $(\text{S}_2)(\text{O}_2)$ complex in Figure 4 based on the present DFT calculations. Strictly speaking, these are Kohn–Sham orbitals and not Hartree–Fock orbitals, and to some extent their physical significance may be questioned. However, Figure 4 clearly shows that only the overall singlet state can produce a stable complex with respect to isolated S_2 and O_2 molecules.

(26) Allen, W. D.; Horner, D. A.; DeKock, R. L.; Remington, R. B.; Schaefer, H. F., III *Chem. Phys.* **1989**, *133*, 11.

(27) Wang, J.; Eriksson, L. A.; Boyd, R. J.; Shi, Z. *J. Phys. Chem.* **1994**, *98*, 1844.

(28) Dixon, D. A.; DeKock, R. L. *J. Chem. Phys.* **1992**, *97*, 1157.

(29) Ignatyev, I. S.; Schaefer, H. F., III *J. Phys. Chem.* **1992**, *96*, 7632.

(30) Murray, C. W.; Laming, G. J.; Handy, N. C.; Amos, R. D. *J. Phys. Chem.* **1993**, *97*, 1868.

(31) DGauss, UniChem 2.3, Cray Research Inc., Mendota Heights, MN.

(32) Andzelm, J.; Wimmer, E. *J. Chem. Phys.* **1991**, *96*, 1280.

(33) Vosko, S. H.; Wilk, L.; Nusair, M. *Can. J. Phys.* **1980**, *58*, 1200.

(34) Becke, A. D. *Phys. Rev. A* **1988**, *38*, 3098. Becke, A. D. *J. Chem. Phys.* **1988**, *88*, 2537.

(35) Perdew, J. P. *Phys. Rev. B* **1986**, *33*, 8822.

(36) Godbout, N.; Salahub, D. R.; Andzelm, J.; Wimmer, E. *Can. J. Chem.* **1992**, *70*, 560.

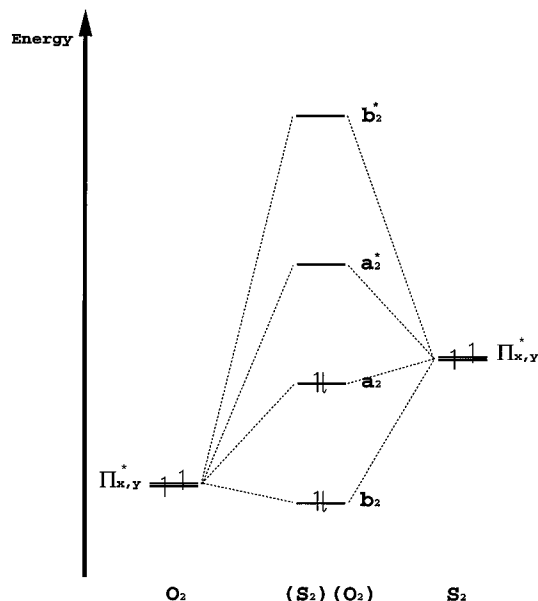


Figure 4. Computed Kohn-Sham MO diagram.

Discussion

The 1403.0-, 725.5-cm⁻¹ and 1404.5-, 391-cm⁻¹ bands are assigned to the (S₂)(O₂) and (Se₂)(O₂) complexes, respectively, based on their formation, spectroscopy, photochemistry, and density functional calculations.

First, the complexes are formed in large yield from super-heater sources of sulfur and selenium where S₂ and Se₂ are the major chalcogen species present. The strong, sharp 1403.0- and 1404.5-cm⁻¹ bands exhibit scrambled ^{16,18}O₂ isotopic triplets strongly suggesting two equivalent oxygen atoms from one oxygen molecule in the complex species. A similar triplet with mixed isotopic sulfur also suggests two equivalent sulfur atoms in the complex.¹³ The 16/18 isotopic ratios, 1.05951 and 1.05984, are indicative of pure O—O stretching motions; the ratio calculated for a pure harmonic motion is 1.06081.

Data for the mixed sulfur-32/sulfur-34 experiment are taken from the earlier study where a 1/2/1 isotopic triplet was observed.¹³ In the current experiments, using sulfur with a natural abundance of isotopes, one band, at 714.9 cm⁻¹ (also observed previously) was found in addition to the 725.5-cm⁻¹ band, and this band had the expected relative intensity for a molecule with two sulfur atoms (~10%). The corresponding (³⁴S₂)(O₂) band is then at 704.1 cm⁻¹, as reported in Table 1 of ref 13. Thus the S—S vibration has the properties expected of a molecule with two equivalent sulfur atoms; here also, the isotopic shift is very near that for isolated S₂; the 32/34 ratio = 1.0295 (1.03074 for harmonic S—S).

By comparison with the fundamental modes for pure O₂ and S₂ (1552 and 717 cm⁻¹, solid argon),^{13,38} respectively, and Se₂ (383 cm⁻¹, gas phase)³⁹ the shifts are quite modest. Moreover, it is noted that the shifts are in opposite directions, to higher

energy for the S—S and Se—Se vibrations and to lower energy for the O—O vibration; this is in accord with expectation in that a shift of electron density from the S₂ and Se₂ moieties to the O₂ moiety would increase the electron density in antibonding O₂ orbitals at the expense of electron density in the similar orbitals in S₂ and Se₂. Within the limitations of the experiment, it was not possible to detect any evidence (i.e., broadening of the middle component of either triplet) of coupling between the O₂ and S₂ moieties; in a mixed oxygen-16/oxygen-18 isotope experiment at moderate resolution, the three components of the O—O stretching motion were all observed to have identical full widths at half maximum absorbance of 2.1 cm⁻¹. These facts are indicative of a weak bond between the S₂ and O₂ subunits.

The matrix electronic spectroscopy described above is consistent with absorption features due to electronic transitions on O₂ and S₂ or Se₂ that are red shifted for O₂ and blue shifted for S₂ or Se₂ transitions. This is in accord with (S₂)(O₂) and (Se₂)(O₂) complexes.

The photochemistry is also supportive of this identification. In the (S₂)(O₂) case, perturbed SO₂ and S₂O are the major photoproducts where the detached atoms remain in the matrix cage and perturb the primary photoproducts. In the (Se₂)(O₂) case, likewise the major photoproducts are perturbed SeO₂ and Se₂O. The Se₂O species will be identified in a detailed study of Se_xO_y species.²⁵

Conclusions

The (S₂)(O₂) and (Se₂)(O₂) complexes have been identified from matrix infrared and electronic spectroscopy using isotopic substitution and found to have symmetrical structures. Red shifts (148–149 cm⁻¹) in the O—O fundamentals and blue shifts in the S—S and Se—Se fundamentals (8 cm⁻¹ each) are in accord with simple transfer of electron density from antibonding π orbitals on S₂ and Se₂ into a like orbital on O₂. Density functional theory calculations found a parallelogram (S₂)(O₂) structure bound by 15 kJ/mol with respect to S₂ and O₂ and predicted a 187-cm⁻¹ red shift for the O—O mode and a 20-cm⁻¹ blue shift for the S—S mode. The latter frequency shifts are in excellent agreement with experiment.

Perhaps the most interesting aspect of this work is to document the formation and weak stability of cyclic (S₂)(O₂) and (Se₂)(O₂) complexes, which do not exist for (O₂)(O₂), but are found for sulfur and selenium as S₄ and Se₄ molecules.

Acknowledgment. We gratefully acknowledge support for this research from the National Science Foundation and helpful discussions with and supporting calculations done by R. King and H. F. Schaeffer, III.

JA960484S

(37) Andrews, L.; Hassanzadeh, P.; Brabson, G. D.; Citra, A.; Neurock, M. *J. Phys. Chem.* **1996**, *100*, 8273.

(38) Andrews, L.; Smardzewski, R. R. *J. Chem. Phys.* **1973**, *58*, 2258.

(39) Huber, K. P.; Herzberg, G. *Constants of Diatomic Molecules*; Van Nostrand Reinhold: New York, 1979.